BIOLOGY OF REPRODUCTION (2016) **94**(1):12, 1–13
Published online before print 2 December 2015.
DOI 10.1095/biolreprod.115.131458

# ALDH Enzyme Expression Is Independent of the Spermatogenic Cycle, and Their Inhibition Causes Misregulation of Murine Spermatogenic Processes[1]

**Travis Kent,[3] Samuel L. Arnold,[4] Rachael Fasnacht,[3] Ross Rowsey,[3] Debra Mitchell,[3] Cathryn A. Hogarth,[3] Nina Isoherranen,[4] and Michael D. Griswold[2,3]**

[3]*School of Molecular Biosciences and the Center for Reproductive Biology, Washington State University, Pullman, Washington*
[4]*Department of Pharmaceutics, University of Washington, Seattle, Washington*

## ABSTRACT

**Perturbations in the vitamin A metabolism pathway could be a significant cause of male infertility, as well as a target toward the development of a male contraceptive, necessitating the need for a better understanding of how testicular retinoic acid (RA) concentrations are regulated. Quantitative analyses have recently demonstrated that RA is present in a pulsatile manner along testis tubules. However, it is unclear if the aldehyde dehydrogenase (ALDH) enzymes, which are responsible for RA synthesis, contribute to the regulation of these RA concentration gradients. Previous studies have alluded to fluctuations in ALDH enzymes across the spermatogenic cycle, but these inferences have been based primarily on qualitative transcript localization experiments. Here, we show via various quantitative methods that the three well-known ALDH enzymes (ALDH1A1, ALDH1A2, and ALDH1A3), and an ALDH enzyme previously unreported in the murine testis (ALDH8A1), are not expressed in a stage-specific manner in the adult testis, but do fluctuate throughout juvenile development in perfect agreement with the first appearance of each advancing germ cell type. We also show, via treatments with a known ALDH inhibitor, that lowered testicular RA levels result in an increase in blood-testis barrier permeability, meiotic recombination, and meiotic defects. Taken together, these data further our understanding of the complex regulatory actions of RA on various spermatogenic events and, in contrast with previous studies, also suggest that the ALDH enzymes are not responsible for regulating the recently measured RA pulse.**

*ALDH, blood-testis barrier, meiosis, retinoic acid, testis*

## INTRODUCTION

Vitamin A metabolism is vital for proper spermatogenesis. Precise regulation of the availability of retinoic acid (RA), the active metabolite of vitamin A, is important for spermatogonial differentiation, blood-testis barrier (BTB) function, meiotic initiation, and proper spermiation (reviewed in [1]). However, the extent of the role that RA plays in regulating these spermatogenic processes or the enzymes and cell types involved in controlling RA levels within the mammalian testis have yet to be fully elucidated. An enhanced understanding of how RA concentrations are regulated within the testis and the complex effects of this molecule on various events during spermatogenesis could have important clinical implications for the treatment of idiopathic male infertility, as well as the development of a safe, effective, and reversible oral male contraceptive.

Retinol, the alcohol form of vitamin A, is transported via serum throughout the body. Once it reaches target tissues, retinol is converted to RA by way of a two-step enzymatic process, the last of which is catalyzed by the aldehyde dehydrogenase (ALDH) enzymes [2]. There are three known RA-synthesizing ALDHs, the transcripts of which have been localized within the murine testis: *Aldh1a1*, *Aldh1a2*, and *Aldh1a3* [3–5]. Thus far, however, reports regarding the localization of these enzymes have been contradictory, incomplete, and focused predominantly on the adult mouse testis. A recent publication reported cell-specific ALDH protein localization in the adult human testis [6], yet the near complete lack of available prepubertal human tissue has meant that the expression and activity of these enzymes during human testis development has remained unclear. A thorough investigation of the ALDH enzymes in both the neonatal and adult testis will help clarify results from contradictory studies and advance our understanding of RA synthesis in the testis throughout development, using the mouse as a model of mammalian spermatogenesis.

There are now multiple lines of evidence to support the hypothesis that RA gradients exist along testis tubules [4, 5, 7], yet there are no data addressing how these gradients are established. Several transcript localization studies have alluded to ALDH1A2 perhaps regulating testicular RA in a pulsatile manner [4, 5], but no quantitative data exist to support this conclusion. Interestingly, the ALDH isozymes have recently been predicted to contribute differently to total testicular RA levels [6, 8]. While 10-fold more ALDH1A1 protein is present in the murine testis compared to ALDH1A2, ALDH1A2 is expected to contribute 61% of the total RA synthesis in the murine testis [8], while, in the human testis, the expected contribution of ALDH1A2 is lower: just 15% [6]. Notably, these studies were performed on whole testis, not in a stage-specific manner, making it impossible to determine if these

[1]This research was supported by National Institutes of Health (NIH) grants R01 10808 to M.D.G., U54 HD 42454 to M.D.G. and N.I., and R01 GM111772 to N.I. and C.A.H. Partial support for this project was funded by National Institute of General Medical Sciences (NIGMS) grant T32 GM083864 to T.K. and National Center for Advancing Translational Sciences (NCATS) grant TL1 TR000422 to S.L.A. The content of this article is solely the responsibility of the authors and does not necessarily represent the official views of the NIGMS or the NIH.
[2]Correspondence: Professor Michael Griswold, School of Molecular Biosciences, P.O. Box 647520, Pullman, WA 99164.
E-mail: mgriswold@vetmed.wsu.edu

Received: 7 May 2015.
First decision: 7 June 2015.
Accepted: 13 November 2015.

eISSN: 1529-7268 http://www.biolreprod.org
ISSN: 0006-3363

differences in isozyme activity contribute to generating RA gradients along testis tubules. A quantitative analysis to measure undulations in ALDH expression and activity along testis tubules is required to determine whether these enzymes are responsible for the proposed RA pulse.

The pulsatility of RA also highlights its importance during spermatogenesis. RA is thought to be vital for several spermatogenic processes, all of which take place when RA levels are highest [1, 7]. The best characterized of these is spermatogonial differentiation, but RA has also been implicated in BTB reorganization, meiotic initiation, and spermiation (see [1, 9] and references therein). The BTB is misregulated in mice with aberrant RA signaling in Sertoli cells [10], and the transcription of *Stra8*, a gene known to be important for proper meiosis [11, 12], is under the direct control of RA [13, 14]. Genes associated with regulating both BTB formation and maintenance, and meiotic initiation and execution have also been shown to be misregulated in RA-deficient models [15].

Due to the complex organization of the testis, the direct study of the mechanisms by which RA controls BTB reorganization, meiotic initiation, and spermiation is difficult. RA-deficient models, as well as their respective RA rescue models, have been used in an attempt to elucidate the roles of this molecule during spermatogenesis [15–25], but have numerous disadvantages. Animals on a vitamin A-deficient (VAD) diet can still release retinol from stored retinyl esters, so an extended length of time is required for the animals to become RA deficient [2]. While it is possible to examine spermatogenesis in animals during induced RA deficiency [16, 20, 21], RA levels were not quantified in these models. As a result, the extent to which dietary induced-deficiency lowers RA levels over time within the testis is unknown, making it difficult to draw conclusions regarding how RA deficiency leads to aberrant spermatogenesis. In addition, once a testis is completely RA deficient, the only germ cells present within the seminiferous tubules are undifferentiated spermatogonia; when RA is reintroduced to this environment, spermatogenesis continues normally, albeit in a synchronous manner [19, 21, 22, 24, 25]. While providing an excellent tool for the study of spermatogonial differentiation, these RA-deprived models are not useful in determining the effects of RA on other spermatogenic processes, such as BTB reorganization and meiotic initiation, as the relevant cell types are not present in the RA-deficient environment. This is of particular importance, because the inhibition of RA synthesis is currently being pursued as a potential nonhormonal, male contraceptive (reviewed in [26]). Treatment with WIN 18 446, a potent inhibitor of RA synthesis, has been shown to inhibit spermatogenesis in a variety of species, but the manner in which spermatogenesis is adversely affected has not been investigated.

The goals of this study were to determine: 1) the cell types that synthesize RA in the developing postnatal murine testis, 2) if ALDHs are responsible for the generation of RA pulses in the testis, and 3) if any spermatogenic defects are associated with this lowered testicular RA environment. Based on ALDH localization, protein quantification, and enzyme activity, the results of this study strongly suggest that ALDH availability is not primarily responsible for the regulation of the RA pulse. Additionally, it is evident that an RA-deficient environment is detrimental to both BTB permeability and meiosis.

## MATERIALS AND METHODS

### Animal Care and Handling

All experiments were conducted using C57BL/6-129 mice following the approval of the Washington State University Animal Care and Use Committee. Mouse colonies were housed in a temperature- and humidity-controlled environment, and food and water was provided ad libitum. Mice were treated as described below and killed by $CO_2$ asphyxiation, followed by either decapitation (0–10 days postpartum [dpp]) or cervical dislocation (>10 dpp). Tissue was dissected from the mouse for further analysis.

### WIN 18 446 and RA Treatments

Spermatogenesis was synchronized as previously described [22]. Briefly, 2 dpp male mice were treated with 100 μg/g body weight WIN 18 446 (a kind gift from Dr. John Amory, University of Washington) or vehicle (1% gum tragacanth) for 7 days. On the following day (eighth day of treatment, 9 dpp), the animals were either killed as WIN 18 446 or vehicle (1% gum tragacanth) only-treated animals or treated with 200 μg all-*trans* RA (atRA) (Sigma-Aldrich), or vehicle (dimethyl sulfoxide). No adverse side effects were witnessed in animals treated with WIN 18 446/RA or vehicle. The animals given injections were then killed at various time points between 1 and 16 days after treatment (induced spermatogenic synchrony) for neonatal analysis or 42–49 days for analysis of synchronized spermatogenesis in the adult testis. For the neonatal time points, pooled testis samples (n = 3 per time point) weighing at least 30 μg each (approximately three animals for 0–4 days posttreatment, two animals for 6 days posttreatment, and one animal for all older time points) were used for ALDH quantification and activity. For each adult animal, one testis was used to determine synchrony by examining the histology across the whole testis and the other was used for ALDH quantification and activity measurements.

To investigate the effects of ALDH inhibition on adult spermatogenesis, adult mice (3–5 mo of age) were treated orally with either 125 mg/kg/day WIN 18 446 or vehicle (1% gum tragacanth) for 1, 8, or 12 days. Animals were killed between 0 and 24 hours after their last dose. The testes were then dissected from these animals and used for RA quantification, biotin permeability assays, meiotic spreads, or RNA sequencing.

### Western Blotting

Western blots were performed using rabbit polyclonal antibodies specific to ALDH1A1 (ab24343, 0.1 μg/ml; Abcam plc), ALDH1A2 (13951-1-AP, 1.3 μg/ml; Proteintech Group), ALDH1A3 (AP7847a, 2.5 μg/ml; Abgent), and ALDH8A1 (sc-130686, 0.1 μg/ml; Santa Cruz Biotechnology). Briefly, equal amounts of adult mouse testis protein was loaded onto and separated via SDS-PAGE (#456-1084; Bio-Rad Laboratories) and transferred to a nitrocellulose membrane. The membrane was then washed briefly with Tris-buffered saline (TBS; 50 mM Tris base, 0.9% NaCl, pH 7.5) and blocked with 5% skim milk in TBS + 0.1% Tween-20 (TBS-T) for 1 h at room temperature. Antibodies were diluted in 5% skim milk/TBS-T and applied to the membranes for approximately 20 h at 4°C. The membranes were then washed three times with TBS-T for 5 min each at room temperature. Secondary antibody (#7074, 1:1000 dilution; Cell Signaling Technology) was applied to membranes for 1 h at room temperature. Membranes were again washed three times with TBS-T for 5 min each before they were imaged via chemiluminescence. The membranes were exposed for between 15 sec and 5 min and imaged on Fujifilm LAS-4000.

### Immunohistochemistry

Immunohistochemistry (IHC) was performed as previously described [27] using mouse testis tissue (n = 3) fixed in Bouin, Davidson, and paraformaldehyde fixative, embedded in paraffin, and sectioned onto charged glass slides using the same antibodies used for Western blotting. Antigen retrieval was achieved using citrate buffer (10 mM, pH 6) at a rolling boil for 5 min. Sections were incubated in primary antibody at a concentration of 0.5 μg/ml (ALDH1A1), 4 μg/ml (ALDH1A2), 2.5 μg/ml (ALDH1A3), or 0.1 μg/ml (ALDH8A1) in 5% normal goat serum/0.1% bovine serum albumin in PBS (137 mM NaCl/2.7 mM KCl/10.1 mM $Na_2HPO_4$/1.8 mM $KH_2PO_4$) at 4°C overnight (~16 h). Control sections were incubated without primary antibody. Biotinylated goat anti-rabbit secondary antibody (956143b; Invitrogen) was applied for 1 h at room temperature, following the manufacturer's instructions. Streptavidin-conjugated horseradish peroxidase (HRP; 956143b; Invitrogen) was also applied for 1 h at room temperature. Binding was determined by a brown precipitate formed by HRP activity in the presence of 3,3′-diaminobenzidine tetrahydrochloride (002020; Invitrogen). Sections were

counterstained with a 1:3 dilution Harris hematoxylin (HHS32-1L; Sigma-Aldrich), dehydrated, and mounted under glass coverslips using DPX mounting media (360294H; VWR International). Cell types were determined using nuclear morphology and location within the testis [28]. Immunostaining paraformaldehyde-fixed sections did not yield convincing staining. Bouin and Davidson fixative both yielded similar localization patterns for all IHC. All histological IHC staining presented in the figures are from Bouin-fixed tissue.

## Generation of Subcellular Fractions from Mouse Tissue

Mouse testis S10 fractions containing microsomes and cytosol were separately generated from 48 samples containing pooled testes from neonatal mice (24–50 mg) and 40 samples containing individual testes from adult mice (43–89 mg), using a previously described method [8]. The total protein concentration in each S10 fraction was measured using a BCA assay (PI-23227; Thermo Scientific).

## Mass Spectrometric Quantification of ALDH Enzymes

The expression of ALDH1A1, ALDH1A2, and ALDH1A3 were quantified in testis S10 fractions using liquid chromatography-tandem mass spectrometry (LC-MS/MS), as described previously, with minor modification [8]. Briefly, the signature peptides used for quantitation were ANNTFYGLAAGLFTK for ALDH1A1, EEIFGPVQEILR for ALDH1A2, and EEIGGPVQPILK for ALDH1A3. To confirm the identification of each ALDH1A in the assay, a second peptide was monitored for each ALDH protein. These second peptides being monitored were VAFTGSTQVGK for ALDH1A1, IFVEESIYEEFVK for ALDH1A2, and ELGEYALAEYTEVK for ALDH1A3. A [$^{13}C_6{}^{15}N_2$]-lysine-labeled ANNTFYGLAAGLFTK peptide was synthesized as an internal standard for ALDH1A1. The internal standard peptides for ALDH1A2 and ALDH1A3 were synthesized as extended versions of the quantification peptide with the sequences VTDDMRIAKEEIFGPVQEILR and EVTDNMRIAKEEIFGPVQ PILK, respectively. These peptides contained a C-terminal [$^{13}C_6{}^{15}N_2$]-arginine and required two cleavages by trypsin to generate the target peptide. Samples were quantified by mass spectrometry using an AB Sciex 5500 qTrap Q-LIT mass spectrometer equipped with an Agilent 1290 UHPLC, as described previously [8]. Each tissue sample was digested in triplicate, as previously described [8], and the resulting peak area for each quantitation peptide was normalized to its corresponding internal standard. The average value of the three digestions was used along with the standard curve for each protein to determine the picomoles of enzyme in each sample. The amount of enzyme in each sample was normalized to the total S10 protein (0.08 mg) in each digestion. All data analysis was performed using Analyst (version 1.5.1; AB Sciex). A signal:noise ratio of 9 was set as the minimum threshold for quantitation.

## Mass Spectrometric Quantification of atRA

The concentrations of atRA in incubations and tissue samples were measured using an AB Sciex 5500 qTrap Q-LIT mass spectrometer equipped with an Agilent 1290 UHPLC, as previously described [7, 8]. For quantification, atRA peak areas were normalized to the atRA-$d_5$ internal standard peak area. All data analysis was performed using Analyst version 1.5.1. A signal:noise ratio of 9 was set as the minimum threshold for quantitation.

## ALDH Activity

To determine atRA formation in testicular S10 protein from mice, the formation of atRA was measured in the testis S10 fractions using previously described methods, with a few modifications [8]. Briefly, 5 μg testicular S10 protein individually from each of the mice was incubated with *at*-retinal at a nominal concentration of 1000 nM in 100 μl of buffer, consisting of 750 mM KCl, 50 mM Hepes, and 2 mM $NAD^+$ at pH 8.0. The incubations were initiated with substrate, performed in triplicate, and terminated after 10 min. The incubations were terminated by transferring 75 μl of the incubation into an equal volume of chilled acetonitrile with 100 nM atRA-$d_5$ (internal standard) and analyzed by LC-MS/MS, as described above. The measured concentration of atRA in each incubation was used to calculate the picomoles of atRA formed per S10 protein (5 μg) per unit time (10 min) to determine the velocity of atRA formation.

## Adult Mouse Testis Staging and Analysis

The stage distribution of both unsynchronized and synchronized animals was determined using previously established guidelines [28–30]. Stage distribution was determined by analyzing greater than 200 tubules from a minimum of two histological cross-sections separated by at least 50 μm in 30 synchronized animals and 10 unsynchronized controls. The midpoint of synchrony, window width, and synchrony factor were determined as previously described [7, 29, 30]. Five animals were excluded from the analysis because samples were lost during preparation or their synchrony factor was less than 3, leaving 25 animals that were included in the analysis.

To determine whether there were statistically significant changes in ALDH levels or activity across the cycle, the samples were divided into three separate bins: before the RA pulse (stages II–VII), during the RA pulse (stages VIII–IX), and after the RA pulse (stages X–I) [7]. Unpaired one-tailed Student *t*-tests were then conducted comparing the samples in a particular bin to all other samples. This was performed for each of the three bins.

## Biotin Permeability Assay

Fresh testes from adult animals treated for 8 days with either WIN 18 446 (n = 4) or vehicle (n = 4) were used to determine the integrity of the BTB, as previously described [31]. Briefly, one testis from each animal was injected with approximately 10% testis weight with PBS containing 1 mM of $CaCl_2$, while the other testis was injected with 10 mg/ml of EZ-Link Sulfo-NHS-LC-Biotin (#21335; Pierce) dissolved in the same solution. The testes were incubated for 30 min in their respective solutions. After incubation, the testes were washed with PBS twice for 5 min each before they were fixed with Bouin fixative for 6 h. The testes were then dehydrated via ethanol wash gradient, mounted in paraffin, and sectioned onto charged glass coverslips. The slides were rehydrated via a graded ethanol wash series and blocked with 5% normal goat serum/0.1% bovine serum albumin in 1× PBS. Streptavidin-conjugated HRP (956143b; Invitrogen) was then applied for 1 h at room temperature. Binding was determined by a brown precipitate formed by HRP activity in the presence of 3,3′-diaminobenzidine tetrahydrochloride (002020; Invitrogen). Sections were counterstained with a 1:3 dilution Harris hematoxylin (Sigma-Aldrich, HHS32-1L), dehydrated, and mounted under glass coverslips using DPX mounting media (VWR International, 360294H). A minimum of 200 tubules was counted for each animal, and permeability was determined based on infiltration of brown staining into the luminal side of the BTB. An unpaired one-tailed Student *t*-test was used to determine statistical significance between WIN 18 446 and control-treated animals.

## Meiotic Preparations and Immunostaining

Testes dissected from adult mice treated with either WIN 18 446 (n = 4) or vehicle (n = 4) for 12 days were placed in PBS. Meiotic preparations were made as described previously [32], with one minor modification: instead of dipping the slide in 1% paraformaldehyde, a thin layer was spread across an uncharged glass slide using a glass Pasteur pipette. Slides were allowed to incubate in a humid chamber overnight, dried, washed in 0.4% Photo-flo 200 solution (Kodak professional), air dried, and immunostained.

For immunostaining, slides were blocked using antibody dilution buffer (ADB; 10 ml normal donkey serum [017-000-001; Jackson Immunoresearch]; 3 g OmniPur bovine serum albumin, Fraction V [9048-40-8; EMD Millipore], 50 μl Triton X-100, and 990 ml PBS, sterile filtered) for 1 h at room temperature. Slides were incubated with SYCP3 antibody (sc-74569, at 0.5 μg/ml; Santa Cruz Biotechnology) and either MLH1 (PC56, at 1.3 μg/ml; Calbiochem) or SYCP1 (nb 300-229, at 10 μg/ml; Novus Biologicals) antibody; MLH1 or SYCP1 primary antibody in ADB was applied to the slide, covered with a glass coverslip, sealed with rubber cement, and incubated at 37°C for approximately 16 h. Following brief ADB wash, SYCP3 primary antibody (diluted in ADB) was applied for 2 h at 37°C under a parafilm coverslip. At the end of the incubation period, slides were washed twice in ADB, 1 h per wash, at room temperature. Alexa Fluor 488-conjugated AffiniPure Donkey Anti-Rabbit secondary antibody (711-545-152; Jackson Immunoresearch Laboratories, Inc.) was then applied to slides before covering with a glass coverslip, sealing with rubber cement, and incubating for approximately 16 h at 37°C. At the end of the incubation, slides were briefly washed with ADB before Cy3-conjugated AffiniPure Donkey Anti-Mouse secondary antibody (715-165-150, at 625 μg/ml; Jackson Immunoresearch Laboratories, Inc.) was applied with parafilm coverslip for 45 min at 37°C. Finally, slides were washed in PBS and mounted with 20 μl of Prolong Gold anti-fade reagent with 4′,6-diamidino-2-phenylindole (P36931; Life Technologies) using glass coverslips. Slides were dried in the dark and stored at 4°C.

## Recombination Analysis

MLH1 foci counts were conducted on 25 pachytene-stage cells per animal by two independent scorers who were blinded with respect to animal status (control vs. treated). Minor scoring discrepancies between scorers were

resolved, and cells with major discrepancies were discarded. Cells with poor staining or synaptic defects were excluded from analysis. An unpaired two-tailed Student *t*-test was conducted to compare the recombination rate in WIN 18 446- and vehicle-treated animals. The number of MLH1 foci per synaptonemal complex (SC) per cell was also assessed. A chi-square analysis was used to determine if the distribution of MLH1 foci along the SCs in the WIN 18 446-treated animals differed significantly from those in the vehicle-treated animals.

### Meiotic Defect Analysis

In a separate analysis, meiotic defects were assessed by assaying 50 pachytene-stage cells per animal using anti-SYCP1 and SYCP3 antibodies to detect SCs. Cells were binned into four categories, as described previously [33]: 1) cells with no detectable meiotic defects, 2) cells with minor synaptic defects (e.g., forks, bubbles, and gaps), 3) cells with major synaptic defects (e.g., partial or complete asynapsis of homologous chromosomes), or 4) cells with telomeric associations between nonhomologous chromosomes. Gaps were defined as a break in SC staining longer than the width of the SC. Forks and bubbles were defined as partial asynapsis, not longer than the width of the SC, at either the distal ends (forks) or internally (bubbles) on the SC. Major defects were defined as either complete asynapsis of homologous chromosomes or asynapsis at least one-third the length of the total SC (partial asynapsis). The frequency of these events was determined in vehicle-treated animals, and a chi-square analysis was performed to determine if the frequency of these events in WIN 18 446-treated animal differed in a statistically significant manner.

## RESULTS

### ALDH Proteins Are Expressed in Different Cell Types in both Neonatal and Adult Mouse Testes

There are very little data regarding ALDH protein expression in either neonatal or adult mouse testes. To rectify this, IHC assays were performed to determine the cellular localization pattern of these RA-synthesizing enzymes within the testis (Figs. 1 and 2). ALDH1A1 localized primarily to Sertoli cells throughout neonatal testis development (Fig. 1, A, E, I, M, Q, and U). ALDH1A2 IHC resulted in immunopositive gonocytes at 0 dpp, but no immunopositive cells at 5 dpp. From 10 dpp onward, spermatocytes and, later, spermatids were immunopositive for ALDH1A2 (Fig. 1, B, F, J, N, R, and V). ALDH1A3 appeared to be diffusely localized to Sertoli cells up to 5 dpp, but shifted to spermatocytes and spermatids by 30 dpp (Fig. 1, C, G, K, O, S, and W). ALDH8A1, a previously uninvestigated RA-synthesis enzyme, was present, but only within Sertoli cells, although not until 30 dpp (Fig. 1, D, H, L, P, T, and X).

The analysis of ALDH enzymes was extended by investigating their localization in the adult testis. Similar to the juvenile testis, both ALDH1A1 and ALDH8A1 were detected predominantly in Sertoli cells (Fig. 2, A and D). ALDH1A2 and ALDH1A3 were present in spermatocytes and round spermatids, while both interstitial cells and elongated spermatids were immunopositive for all four ALDH enzymes. Interestingly, ALDH8A1 was the only ALDH enzyme that appeared to be present in spermatogonia, although some spermatogonia were ALDH8A1-negative (Fig. 2D, green arrow and asterisks, respectively). Western blots were performed with the ALDH antibodies to ensure specificity (Supplemental Fig. S1; all Supplemental Data are available online at www.biolreprod.org).

### Expression of ALDH Enzymes Does Not Cycle in the Same Manner as RA

Stage-specific expression of the ALDH enzymes was not visualized via IHC, as this assay only provides qualitative data. To obtain quantitative information regarding the expression of the ALDH enzymes during the first wave of spermatogenesis and across the cycle of the seminiferous epithelium, spermatogenesis was synchronized using the WIN 18 446/RA treatment protocol [22]. Samples from both synchronized and unsynchronized vehicle control-treated animals were assayed for ALDH1A1, ALDH1A2, and ALDH1A3 protein levels (Fig. 3A). Using a novel tandem HPLC-MS/MS [8] on synchronized testes during the first wave of spermatogenesis in juvenile mice, we found that the enzyme present at the highest level was ALDH1A1 (Fig. 3B). ALDH1A1 levels fell from 600 to 200 pmol/mg of S10 protein from 0–16 days after the neonatal synchrony protocol, with no statistical differences between synchronized and unsynchronized samples. Conversely, the highest levels of ALDH1A2 protein, approximately 15–17 pmol/mg of S10 protein, were observed later during development: 14 days after synchrony treatment in the juvenile testis (Fig. 3C). There was no statistical significance between the levels of ALDH1A2 protein in synchronized and unsynchronized samples, except at 4 and 12 days posttreatment, where ALDH1A2 levels were observed to be lower than controls. In both the synchronized and unsynchronized samples, ALDH1A3 concentrations were below 1.3 pmol/mg testicular S10 protein (data not shown).

This analysis was extended to synchronized adult spermatogenesis to determine if stage-specific cycling of ALDH enzyme levels was occurring. Overall, ALDH1A1 and ALDH1A2 levels varied from ~80–180 pmol/mg and ~10–20 pmol/mg of S10 protein, respectively (Fig. 3, D and E). ALDH1A3 concentrations were, again, below 1.3 pmol/mg S10 protein (data not shown). To determine whether ALDH protein levels varied significantly across the spermatogenic cycle, samples were binned into three categories for further analysis. In creating categories, we were interested in assessing ALDH levels before, during, and after the RA peak described previously [7]. If the ALDH enzymes are responsible for testicular RA pulsatility, the enzymes should be most abundant prior to the peak of RA and least abundant just after the peak. We therefore established our three categories as stages II–VII (before), stages VIII–IX (during), and stages X–I (after). In the case of both ALDH1A1 and ALDH1A2, there was no significant difference in ALDH protein levels either before, during, or after the RA peak (Fig. 3).

### ALDH Activity Does Not Undergo Cyclic Changes

Neither IHC nor protein quantification displayed stage-specific expression of ALDH enzymes, yet it is known that RA is present in a stage-specific manner [7]. To further investigate whether the ALDH enzymes are responsible for the stage-specific availability of RA, total ALDH activity across the spermatogenic cycle was determined using HPLC-MS/MS (Fig. 4). Samples were again binned and compared, as described for the ALDH enzyme levels, and showed no changes in ALDH activity before, during, and after the pulse of RA.

### ALDH Inhibition Across One Spermatogenic Cycle Significantly Lowers Testicular RA Levels

In addition to characterizing the ALDH enzymes, we also investigated the effects of ALDH inhibition on various aspects of spermatogenesis, as a follow up to previous studies [22, 34]. To better understand the effects of WIN 18 446 on testicular RA levels, animals were treated for 8 days with 125 mg/kg/day of WIN 18 446. Animals were killed at various time points within a 24-hour window following the first and eighth dose. HPLC-MS/MS measurements following a single dose of WIN

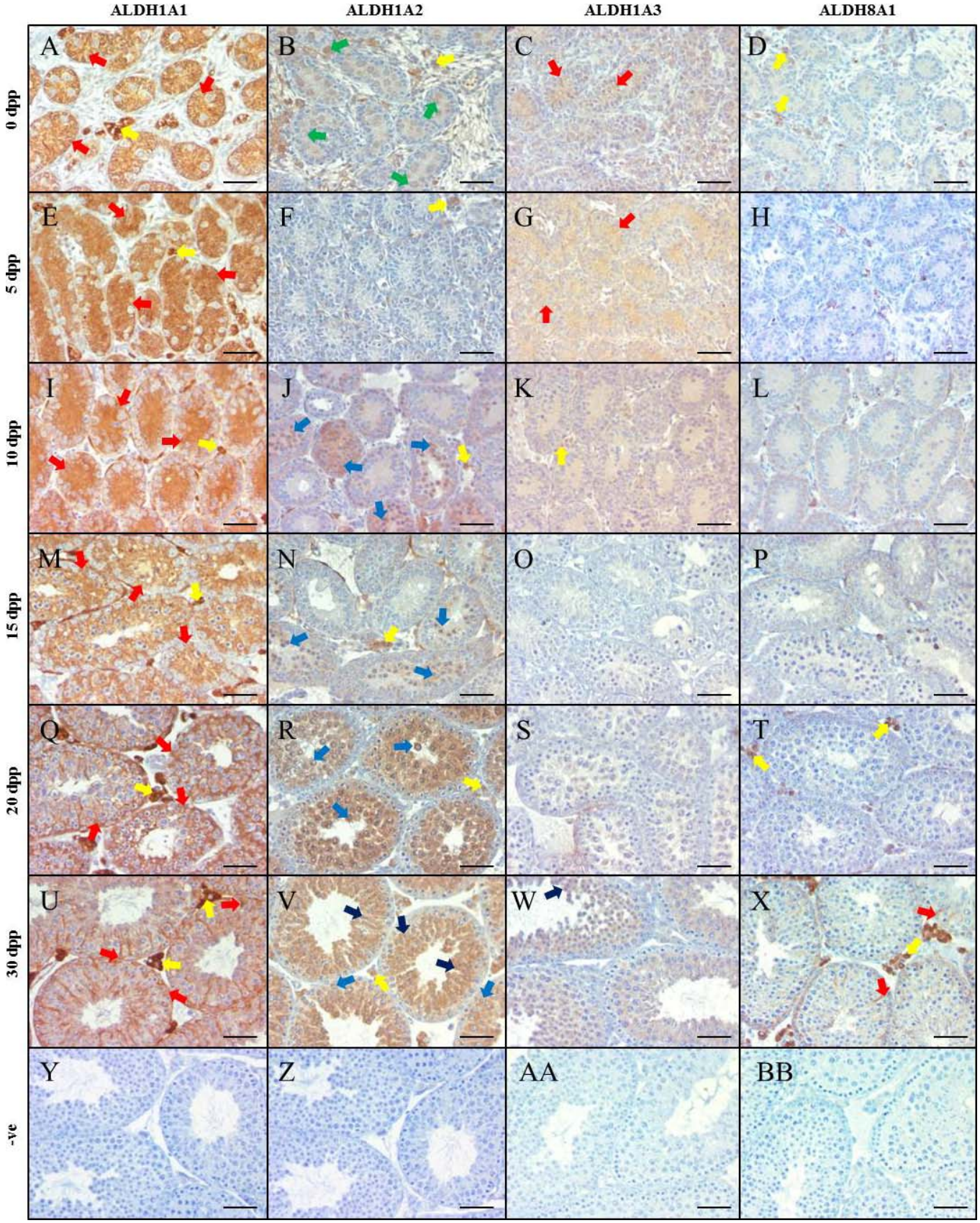


FIG. 1. ALDH enzymes are differentially localized in the neonatal murine testis. Images are representative murine testicular cross-sections displaying IHC analysis of ALDH localization at various neonatal ages. ALDH1A1 is represented in **A**, **E**, **I**, **M**, **Q**, and **U** for 0, 5, 10, 15, 20, and 30 dpp, respectively. ALDH1A2 is represented in **B**, **F**, **J**, **N**, **R**, and **V**, while ALDH1A3 is represented in **C**, **G**, **K**, **O**, **S**, and **W** for the same time points. Finally, ALDH8A1 is displayed in **D**, **H**, **L**, **P**, **T**, and **X**. Negative controls (–ve) are shown in **Y-BB**. Brown staining indicates an immunopositive reaction. Arrows indicate immunopositive cells, while the respective colors indicate the following cell types: red, Sertoli cells; yellow, Leydig/interstitial cells; dark blue, spermatid; light blue, spermatocyte; green, gonocyte/spermatogonia. Bars = 100 μm.

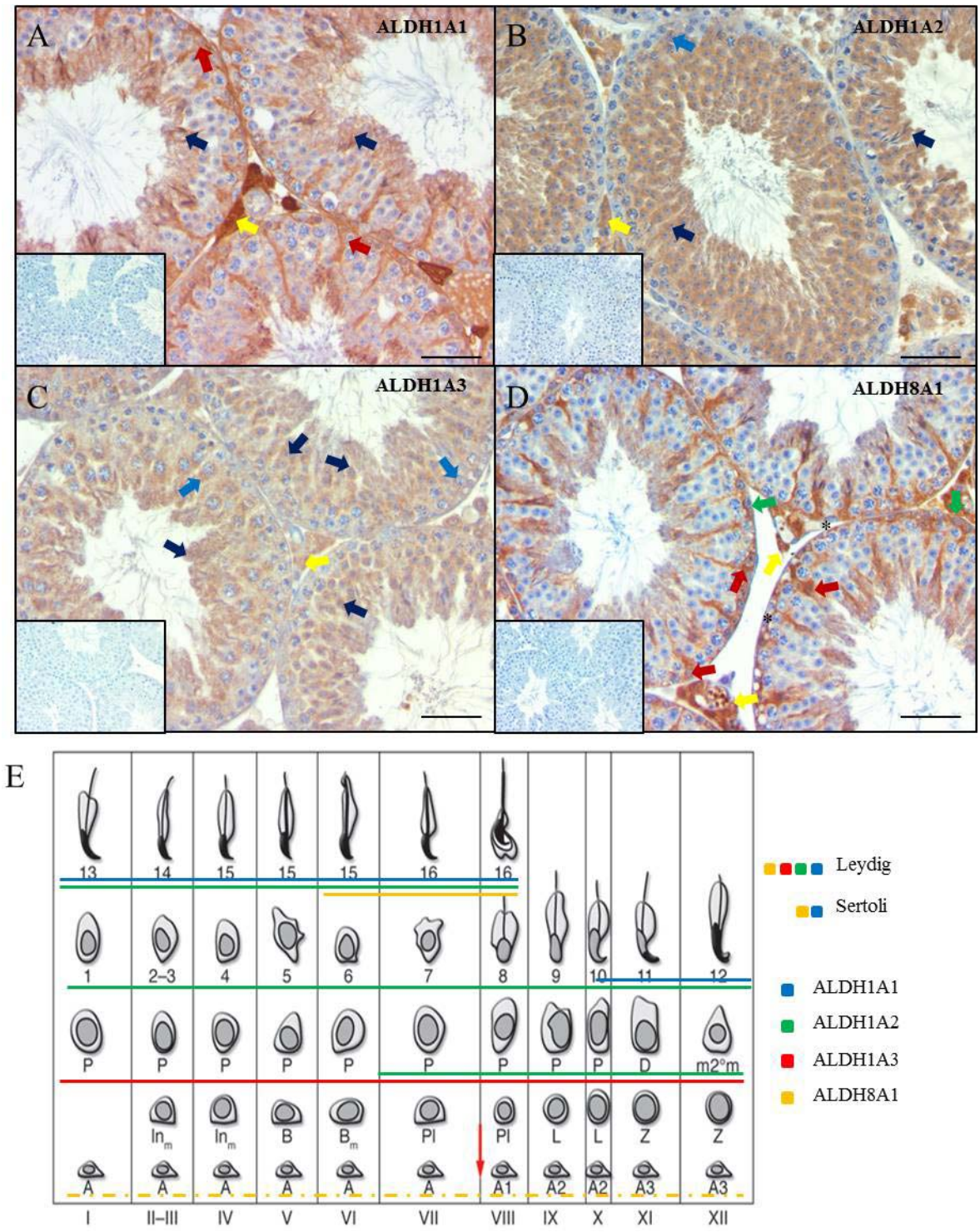


FIG. 2. ALDH enzymes locate to different cell types in the adult murine testis. Images are representative adult murine testicular cross-sections displaying IHC analysis of ALDH localization. ALDH 1A1, -1A2, -1A3, and -8A1 localization can be seen in **A**, **B**, **C**, and **D**, respectively. Negative controls for each assay are shown in the picture inserts. Brown staining indicates an immunopositive reaction. Arrows indicate immunopositive cells, while the respective colors indicate the following cell types: red, Sertoli cells; yellow, Leydig/interstitial cells; dark blue, spermatid; light blue, spermatocyte; green, gonocyte/spermatogonia. Asterisks represent immunonegative spermatogonia. Bars = 100 μm. A summary of the adult localization data is presented in **E**. A solid line underneath a cell indicates that the cell is immunopositive for the respective ALDH. ALDH1A1, -1A2, -1A3, and -8A1 are represented by blue, green, red, and yellow, respectively. Stage diagram adapted from Hogarth and Griswold [64] with permission of the American Society for Clinical Investigation.

18 446 showed a 63% reduction in testicular RA concentrations (Fig. 5A). An 8-day WIN 18 446 treatment also resulted in lowered testicular RA levels to an average of 20% of control (Fig. 5B), consistent with previous studies [8, 22, 34].

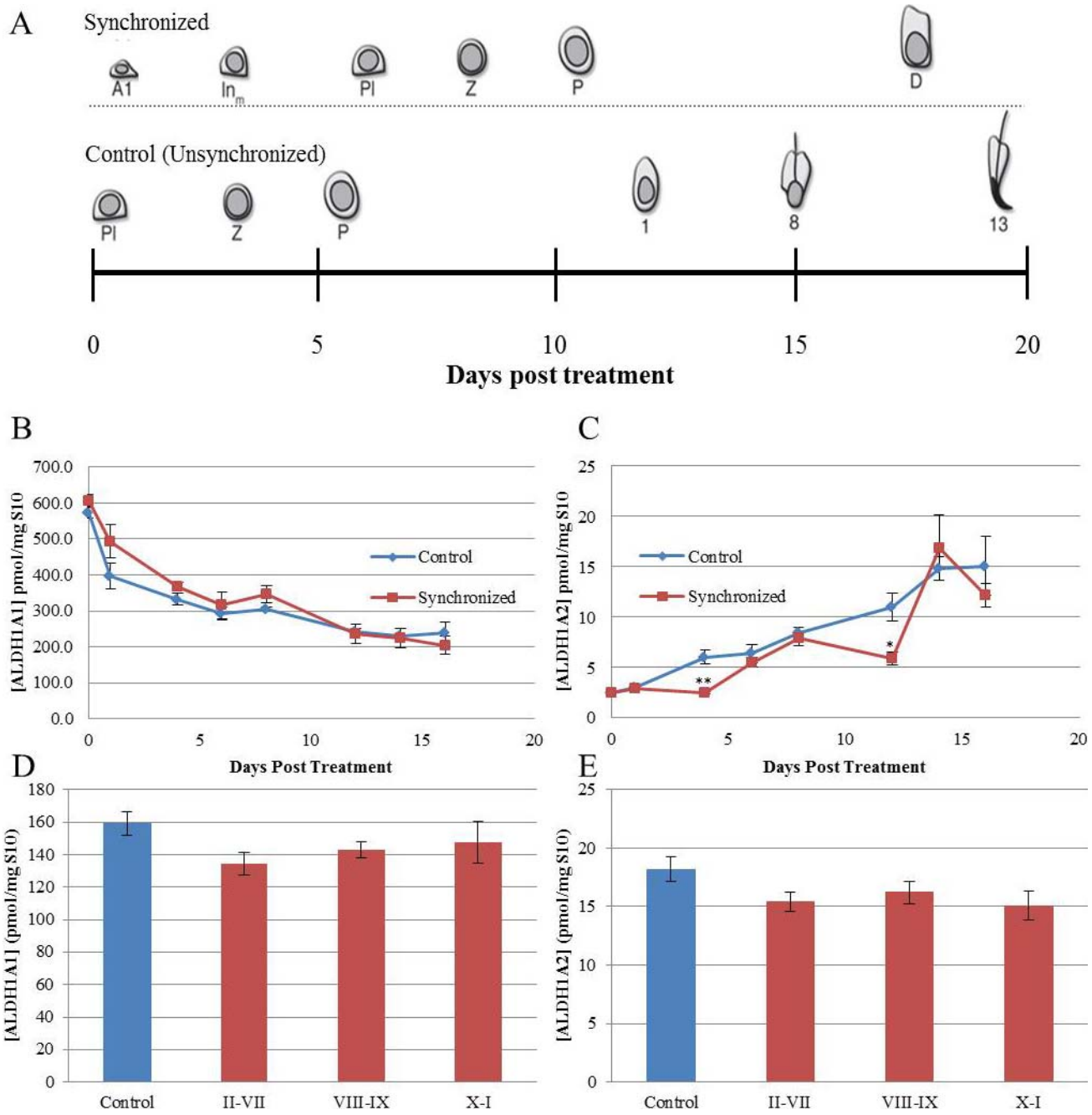


FIG. 3. ALDH1A1 and ALDH1A2 levels do not vary in a manner similar to RA. **A** represents the cell types entering the testicular environment following synchrony protocol (top row) or control (bottom row). ALDH1A1 (**B** and **D**) and ALDH1A2 (**C** and **E**) protein levels were quantified in both synchronized (red) and control (blue) animals using a tandem HPLC-MS/MS approach. In the neonatal analysis (**B** and **C**), the vertical axis represents ALDH protein/mg of S10 protein. The horizontal axis represents time following neonatal synchrony treatment. Vertical error bars represent the SEM. Student *t*-tests were used to compare the protein levels in synchronized and control animals ($^{*}P < 0.05$, $^{**}P < 0.01$). In the synchronized adult analysis (**D** and **E**), 25 animals were collected at 12-h intervals between 42 and 50 days postsynchrony. The midpoint of synchrony was determined and used to bin each sample into three categories (stages II–VII, stages VIII–IX, and stages X–I). ALDH protein/mg of S10 protein was determined and averaged for both the unsynchronized controls (blue) and the three bins (red). The vertical control error bar is representative of the SEM for each category. ALDH1A3 levels were measured in both the adult and neonatal testis, but were at concentrations below the threshold of detection.

### *The BTB Is Significantly Altered in Mice Treated with WIN 18 446*

To determine the effects of this lowered testicular RA environment on the BTB, we performed a biotin-permeability assay on mice treated for 8 days with either WIN 18 446 or vehicle control. This functional assay allows for the detection of tubules with a disrupted BTB by probing for a biotin tracer molecule that was injected into freshly dissected testes (Fig. 6, A and B). There was a small, but statistically significant, increase in permeable tubules in animals treated with WIN 18 446 (4.8%) compared to controls (2.7%) (Fig. 6C).

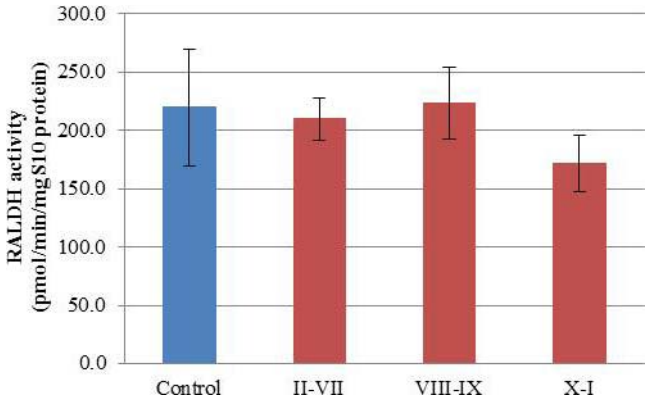


FIG. 4. ALDH activity does not undergo cyclic changes. The graph represents mean ALDH activity (y-axis) within each category. The four categories used were: control (blue), stages II–VII, stages VIII–IX, and stages X–I (red). Error bars are representative of the SEM for each category.

### *WIN 18 446 Treatment Affects Meiotic Recombination and the Frequency of Synaptic Defects*

Because RA has been implicated in playing a role during meiotic initiation [11–14, 35, 36], we investigated whether meiosis was altered in animals treated with WIN 18 446. Animals were treated for 12 days with WIN 18 446 to ensure that spermatocytes analyzed at pachytene had initiated meiosis in a testicular environment with lowered RA. Meiotic preparations were immunostained for SYCP3 and MLH1, markers for the SC and sites of recombination, respectively (Fig. 7, A and B). The number of MLH1 foci in pachytene spermatocytes was quantified in WIN 18 446-treated animals (26.22 ± 0.26 MLH1 foci/cell) and controls (25.39 ± 0.28 MLH1 foci/cell) (Fig. 7C). A statistically significant increase in MLH1 foci was detected in WIN 18 446-treated animals compared to controls. To extend our recombination analysis, the distribution of foci across the genome was assessed by analyzing the number of ''recombinationless'' chromosomes; no significant difference was detected between WIN 18 446-treated and control animals (Fig. 7C).

In addition to aberrant recombination, meiotic defects can also cause a cell to undergo apoptosis, thereby adversely affecting fertility [37, 38]. Thus, to determine if lowered testicular RA levels increased the frequency of meiotic defects, we quantified these defects in pachytene cells immunostained for SYCP1 and SYCP3. Defects were separated into three categories—associations, minor defects, and major defects—and representative images of normal and abnormal cells are shown in Figure 8, A–D. Our analysis revealed a significant increase in all three classes of defects in spermatocytes from WIN 18 446-treated animals by comparison to controls, and a statistically significant decrease in cells with no synaptic defects (Fig. 8E).

## DISCUSSION

This report provides the first comprehensive analysis of the ALDH proteins in the murine testis through postnatal development, as well as a thorough investigation into the effects of short-term inhibition of these RA-synthesizing enzymes on various aspects of spermatogenesis. Here, we show that the ALDH enzymes are likely not primarily responsible for endogenous RA pulsatility, but that the inhibition of these enzymes has adverse effects on BTB permeability and proper meiotic function through reduced intratesticular RA concentrations.

While there have been a multitude of studies regarding the effects of ALDH inhibition via WIN 18 446 treatment on fertility [22, 39–45], it is not yet clear through which mechanisms ALDH inhibition compromises spermatogenesis. Consistent with previous reports [8, 34], we show that our treatment regime with WIN 18 446 causes an 80% reduction in testicular RA levels, allowing for a more thorough investigation of how spermatogenesis proceeds in a lowered, but not deficient, RA environment. While spermatogonial differentiation is the best-characterized spermatogenic event known to be under RA control [17–25, 46–48], there is evidence that RA is also important in BTB maintenance [10, 15, 49–52]. Several key genes coding for proteins integral to the BTB are misregulated in VAD mice [15]. Additionally, Sertoli cells cultured in the presence of RA display increased expression of transcripts coding for proteins vital for BTB integrity, such as *Tjp1* and *Cldn11* [51]. Finally, BTB permeability was compromised in animals with testes treated with a Sertoli cell-specific dominant-negative RA receptor lentivirus [10].

The data presented here show that a lowered testicular RA environment induces a mild increase in BTB permeability. While the increase in permeability reached statistical significance, we were surprised that this increase was not more drastic. It is possible that an 80% reduction in RA

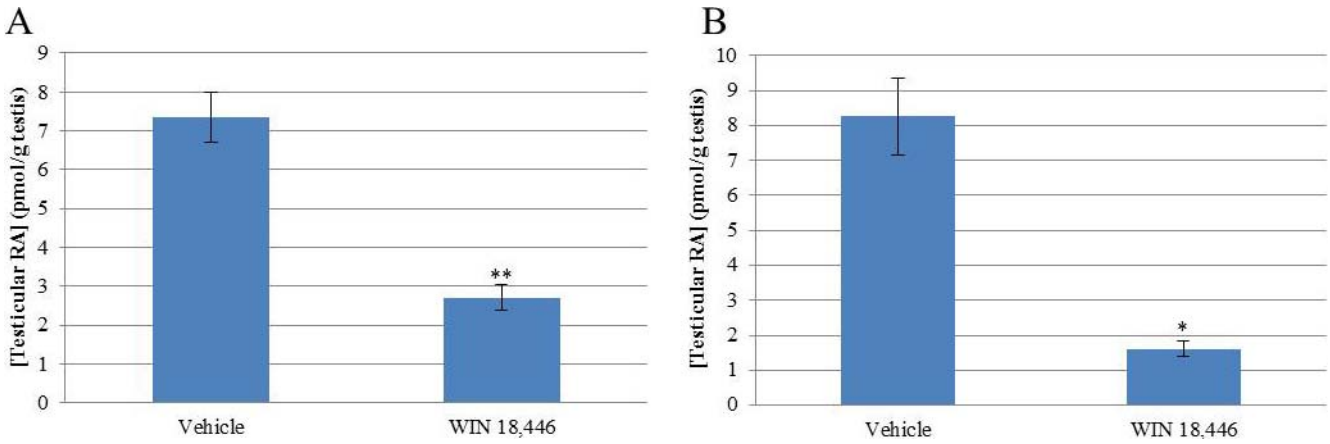


FIG. 5. Animals treated with WIN 18 446 have lowered testicular RA levels. Adult mice were treated daily with WIN 18 446 for either 1 (**A**) or 8 (**B**) days (n = 24). Their testes were collected within a 24-h window of the final treatment. The RA levels were measured (y-axis), and a Student *t*-test was used to determine statistical significance (*$P < 0.05$, **$P < 0.01$).

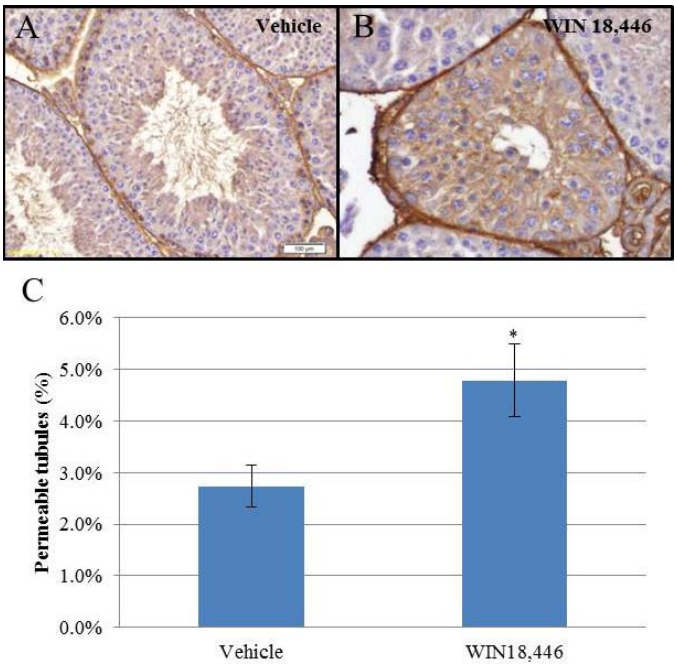


FIG. 6. Blood-testis barrier permeability is adversely affected in animals treated with WIN 18 446. Adult mice (n = 4) were treated daily with WIN 18 446 for 8 days. BTB integrity was assessed using a biotin permeability assay. Representative images of a tubule with an intact BTB and a compromised BTB are shown in **A** and **B**, respectively. Brown staining is indicative of the presence of the biotin tracer. Bar = 100 μm. The percentage of permeable tubules was determined for each treatment, and a Student *t*-test was used to determine statistical significance (**C**) (*$P < 0.05$).

concentration was not sufficient to completely eliminate proper BTB function. While the biological significance of this mild decrease in BTB permeability is not currently known, further exposure to a low testicular RA environment could exacerbate this phenotype. The change in BTB permeability after such a short exposure to WIN 18 446 is suggestive of this being one of the first structures susceptible to a low testicular RA environment. Because BTB permeability has been shown to be vital for proper testis function [31], any misregulation of the BTB would likely have reproductive consequences.

RA has also been implicated in playing a vital role during meiosis [11–14, 22, 36]. Animals lacking *Stra8*, a gene known to be stimulated by RA [13, 14], fail to properly undergo meiosis [11, 12], indicating that this RA-responsive gene is important for meiotic progression. The data presented here show, for the first time, that germ cells are not only able to initiate meiosis in a low testicular RA environment, but also have an increased recombination rate and an increase in both major and minor meiotic defects. While the biological significance of the increase in meiotic recombination is not fully understood, it is known that increases in meiotic defects can be detrimental to viable sperm production [33, 37, 38]. Specifically, it has been shown that a one-focus increase in recombination correlates with a 10% reduction in cells exiting meiosis [33]. This, in conjunction with the 10% increase in cells with major defects, could result in a potential reduction of cells exiting meiosis. When taken together, these data provide support for the hypothesis that RA plays a role in proper meiotic regulation, but that meiotic initiation can still take place in a lowered testicular RA environment.

While there have been multiple studies investigating the effects of WIN 18 446 on spermatogenesis [22, 39–45], fewer data have been published regarding the regulation of this molecule's target enzymes: the ALDHs. Recent transcript localization studies have led to the hypothesis that ALDH enzyme activity varies across the spermatogenic cycle, driving

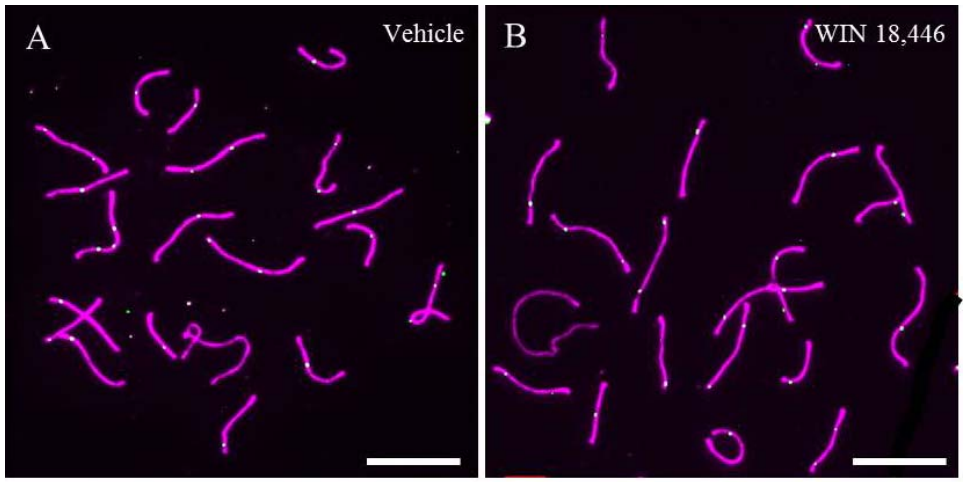


| C | Mean MLH1 foci/cell | e0 | e1 | e2 | e3 |
|---|---|---|---|---|---|
| Vehicle | 25.39 ± 0.283 | 2.05% | 62.84% | 34.53% | 0.58% |
| WIN 18,446 | 26.22 ± 0.261* | 0.84% | 60.74% | 38.00% | 0.42% |

FIG. 7. WIN 18 446 treatment increases recombination rate. Animals (n = 4) were treated with WIN 18 446 for 12 days. Meiotic spreads and IHC were performed to determine recombination rates. **A** and **B**) Representative images of cells from control and WIN 18 446-treated animals, respectively. Purple and green staining are representative of SYCP3 and MLH1, respectively. e0, e1, e2, and e3 denote the percentage of chromosomes containing 0, 1, 2, and 3 exchanges, represented by MLH1. **C**) A Student *t*-test was used to determine if there was a statistically significant difference in recombination rate between control and WIN 18 446-treated animals (*$P < 0.05$). Bar = 10 μm.

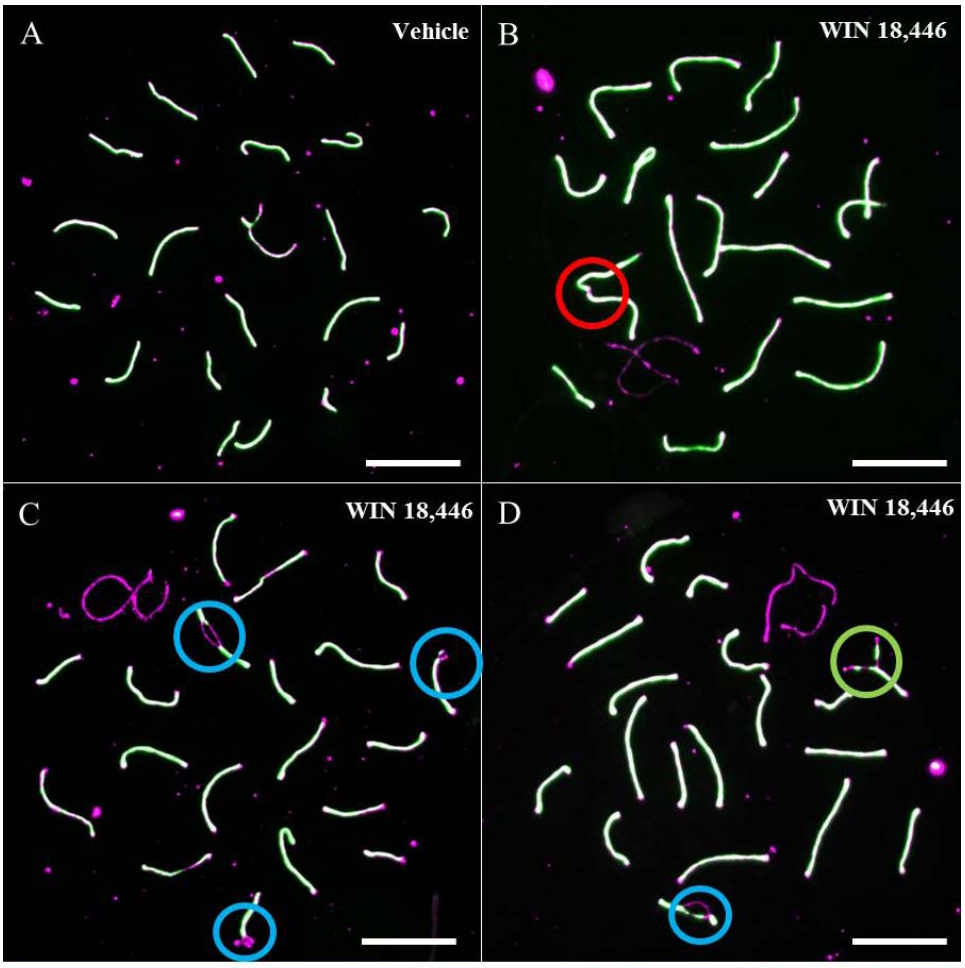


| E | Perfect | Minor | Major | Associations |
|---|---|---|---|---|
| Vehicle | 82.5% | 3.0% | 8.0% | 10.0% |
| WIN 18,446 | 68.5% | 6.5% | 18.0% | 13.5% |

p= 0.003

FIG. 8. WIN 18 446 induces meiotic defects. Animals (n = 4) were treated daily with WIN 18 446 for 12 days. Meiotic spreads and IHC were performed to assess meiotic defects. Purple and green staining are representative of SYCP3 and SYPC1, respectively. Cells were binned into four categories 1) cells with no detectable meiotic defects (**A**), 2) cells containing association of two nonhomologous chromosomes at their distal ends (**B**), 3) cells with minor synaptic defects, such as forks, bubbles, and gaps (**C**), or 4) cells with major synaptic defects, such as partial or complete asynapsis of homologous chromosomes (**D**). The circles highlight the specific meiotic defects in each cell, with red representing associations, blue representing minor defects, and green representing major defects. **E**) The percentage of cells containing each defect. The values do not add up to 100%, because some cells, such as the one depicted in **D**, displayed two different types of defects. Bar = 10 μm.

the RA pulse [4, 5, 53]. These localization data, however, are incomplete and contradictory, focusing primarily on transcript localization in the adult murine testis. Here, we present, for the first time, a comprehensive localization of four ALDH enzymes in the postnatal testis. Our findings show that ALDH1A1 is present in the Sertoli and Leydig cells (Figs. 1 and 2), agreeing with the transcript localization observed by Vernet et al. [4] and the protein localization in the human testis [6]. ALDH8A1, known to be present in the human testis and capable of synthesizing RA [54], was similarly localized to both Sertoli and Leydig cells (Figs. 1 and 2). Almost no information is known about the activity of ALDH8A1 in vivo, and future studies are required to determine the contribution of this enzyme to testicular RA synthesis, especially in murine models where the activity of the more well-characterized isozymes has been perturbed [24]. ALDH1A2 localized predominately to the meiotic and postmeiotic germ cells in the adult testis (Fig. 2); however, it was not expressed in a stage-specific manner, as has been previously reported [4, 5, 55]. Vernet et al. [4] reported *Aldh1a3* transcript localization in the Leydig cells, which we were able to confirm at the protein level (Fig. 2). In the adult testis, we also were able to detect ALDH1A3 protein in late spermatocytes and round spermatids (Fig. 2). Importantly, the localization patterns of the two enzymes predicted to contribute the most to testicular RA synthesis in both the mouse and the human, ALDH1A1 and ALDH1A2, were conserved between these two species [6, 8].

To determine if the ALDH enzymes play a role in RA cyclicity, ALDH IHC, quantification, and activity were assessed in both the developing and adult testis. ALDH1A1 protein levels drop throughout juvenile testis development, and do not vary significantly across the cycle (Fig. 3), matching the

IHC Sertoli cell localization data for this enzyme perfectly (Fig. 1). As the numbers of germ cells within the testis increase during development, the relative abundance of the Sertoli cells, where ALDH1A1 is predominantly localized, drops. IHC analysis of ALDH1A1 in the adult also demonstrated that this isozyme is present in every tubule (Fig. 2), consistent with the protein quantification data (Fig. 3). While it is known that RA synthesis within Sertoli cells is necessary for spermatogonial differentiation in the neonatal testis [24], *Aldh1a1*-null mice are both viable and fertile [56], indicating that ALDH1A1 is not required for this process.

While ALDH1A2 protein levels did increase throughout juvenile testis development, they remained constant across adult spermatogenesis. Due to the synchrony protocol utilized for protein quantification, the testes of the synchronized animals were developmentally delayed by ~7 days compared to controls [22, 57]. Therefore, the significant differences in observed in ALDH1A2 protein level between controls and synchronized developing testes are likely the result of new, ALDH1A2-expressing cell types entering the testicular milieu in the unsynchronized controls. Specifically, the observed, statistically significant differences correspond nicely with the appearance of preleptotene spermatocytes and round spermatids in the unsynchronized controls, cell types that are not present in the corresponding synchronized animals, at 4 and 12 days posttreatment, respectively. It is not likely that these increases were responsible for RA pulsatility, as the drastic changes seen in RA levels in synchronized neonatal animals [7] were not observed in ALDH1A2 levels. As was observed with ALDH1A1, ALDH1A2 protein levels did not change significantly in a stage-specific manner in the adult testis, matching the corresponding IHC data (Fig. 3). Since ALDH1A3 levels were not detected via HPLC-MS/MS analysis, we were not able to detect stage specificity when analyzing protein localization. However, based on the activity of ALDH1A3 and its low expression levels, this enzyme is predicted to contribute less than 5% to total RA levels synthesized within either the human or mouse testis [6, 8], and is unlikely to regulate cyclic RA concentrations.

In addition to protein localization and quantification of ALDH enzymes across the cycle, stage-specific ALDH enzyme activity during adult spermatogenesis was also not detected in our assays. When viewed as a whole, the data presented in this current study strongly suggest that the pulsatile RA concentrations recently measured within testis tubules [7] are likely not the result of stage-specific ALDH activity. However, despite the multiple approaches taken to investigate whether these enzymes contribute to the pulse, there are still limitations associated with our techniques and, therefore, we cannot definitively rule out ALDH as regulating testicular RA levels in a pulsatile manner. These limitations include the nonquantitative nature of IHC analyses and the fact that the mass spectrometry protein quantification and enzyme activity assays were performed on the S10 fraction of whole testes, not within the seminiferous tubules themselves. However, despite these technical inadequacies, the data presented here do indicate that the ALDH enzymes are not responsible for the RA pulse.

If the ALDH enzymes are not regulating pulsatile RA levels within testis tubules, then what is? RA concentrations are usually maintained in a very narrow range by balancing synthesis with degradation. The CYP26 enzymes are known to degrade RA, but whether their expression or activity is stage specific either remains up for debate or is undetermined [4, 5, 55]. A second possibility is that the ALDH substrate, retinaldehyde, is provided in a pulsatile manner. The overall rate of RA biosynthesis is determined by the conversion of retinol to retinaldehyde [58], and there are several recent studies to demonstrate that the opposing, yet coordinated, activities of the retinol dehydrogenase and reductase enzymes are critical for maintaining RA homeostasis [59–62]. The notion that this is also occurring across the cycle of the seminiferous epithelium is supported by the observation that a member of each of these gene families, *Rdh10* and *Dhrs4*, is expressed in a stage-specific manner, peaking either when or just after RA levels are highest [7].

In addition to regulation at the ALDH substrate level, retinol availability may also be pulsatile. LRAT, the only known retinol esterase, is responsible for the conversion of retinol to retinyl esters for storage within cells [63]. Stage-specific expression of *Lrat* has been detected in separate studies [5, 7], with levels highest in stages II–VI, prior to the pulse, implying that retinoid storage, rather than RA synthesis, is promoted during the stages when RA levels are lowest. Taken together, a model can be postulated whereby either retinol or retinaldehyde is available in a pulsatile manner along testis tubules, and steady-state ALDH levels across the cycle allow for RA to be generated quickly in response to rising retinaldehyde levels. Quantitative analyses of the CYP26 and the retinol dehydrogenase/reductase enzymes in a stage-specific manner and determining which testicular cell types contribute to generating the RA pulse will be the focus of our future studies.

It is clear that RA acts as more than just an on/off switch for spermatogonial differentiation. Here, we provide evidence that a lowered testicular RA environment compromises BTB integrity, as well as increases the number of meiotic defects, both of which have been shown to have an adverse effect on fertility. It will be important for future studies to determine if these spermatogenic defects are present in men with lowered testicular RA levels, and if these defects can be rescued via pharmaceutical intervention.

## ACKNOWLEDGMENT

The authors would like to thank Dr. Mary Zoulas of the Seattle Animal Shelter for kindly providing dog testicular tissue for controls, and Dr. John Amory (University of Washington) for providing the WIN 18 446.

## REFERENCES

1. Kent T, Griswold MD. Checking the pulse of vitamin A metabolism and signaling during mammalian spermatogenesis. J Dev Biol 2014; 2:34–49.
2. Theodosiou M, Laudet V, Schubert M. From carrot to clinic: an overview of the retinoic acid signaling pathway. Cell Mol Life Sci 2010; 67: 1423–1445.
3. Zhai Y, Sperkova Z, Napoli JL. Cellular expression of retinal dehydrogenase types 1 and 2: effects of vitamin A status on testis mRNA. J Cell Physiol 2001; 186:220–232.
4. Vernet N, Dennefeld C, Rochette-Egly C, Oulad-Abdelghani M, Chambon P, Ghyselinck NB, Mark M. Retinoic acid metabolism and signaling pathways in the adult and developing mouse testis. Endocrinology 2006; 147:96–110.
5. Sugimoto R, Nabeshima Y, Yoshida S. Retinoic acid metabolism links the periodical differentiation of germ cells with the cycle of Sertoli cells in mouse seminiferous epithelium. Mech Dev 2012; 128:610–624.
6. Arnold SL, Kent T, Hogarth CA, Schlatt S, Prasad B, Haenisch M, Walsh T, Muller CH, Griswold MD, Amory JK, Isoherranen N. Importance of ALDH1A enzymes in determining human testicular retinoic acid concentrations. J Lipid Res 2015; 56:342–357.
7. Hogarth CA, Arnold S, Kent T, Mitchell D, Isoherranen N, Griswold MD. Processive pulses of retinoic acid propel asynchronous and continuous murine sperm production. Biol Reprod 2015; 92:37.
8. Arnold SL, Kent T, Hogarth CA, Griswold MD, Amory JK, Isoherranen N. Pharmacological inhibition of ALDH1A in mice decreases all-*trans* retinoic acid concentrations in a tissue specific manner. Biochem Pharmacol 2015; 95:177–192.
9. Mark M, Teletin M, Vernet N, Ghyselinck NB. Role of retinoic acid

receptor (RAR) signaling in post-natal male germ cell differentiation. Biochim Biophys Acta 2015; 1849:84–93.
10. Hasegawa K, Saga Y. Retinoic acid signaling in Sertoli cells regulates organization of the blood-testis barrier through cyclical changes in gene expression. Development 2012; 139:4347–4355.
11. Anderson EL, Baltus AE, Roepers-Gajadien HL, Hassold TJ, de Rooij DG, van Pelt AM, Page DC. Stra8 and its inducer, retinoic acid, regulate meiotic initiation in both spermatogenesis and oogenesis in mice. Proc Natl Acad Sci U S A 2008; 105:14976–14980.
12. Mark M, Jacobs H, Oulad-Abdelghani M, Dennefeld C, Feret B, Vernet N, Codreanu CA, Chambon P, Ghyselinck NB. STRA8-deficient spermatocytes initiate, but fail to complete, meiosis and undergo premature chromosome condensation. J Cell Sci 2008; 121:3233–3242.
13. Bouillet P, Oulad-Abdelghani M, Vicaire S, Garnier JM, Schuhbaur B, Dolle P, Chambon P. Efficient cloning of cDNAs of retinoic acid-responsive genes in P19 embryonal carcinoma cells and characterization of a novel mouse gene, Stra1 (mouse LERK-2/Eplg2). Dev Biol 1995; 170: 420–433.
14. Oulad-Abdelghani M, Bouillet P, Decimo D, Gansmuller A, Heyberger S, Dolle P, Bronner S, Lutz Y, Chambon P. Characterization of a premeiotic germ cell-specific cytoplasmic protein encoded by Stra8, a novel retinoic acid-responsive gene. J Cell Biol 1996; 135:469–477.
15. Chihara M, Otsuka S, Ichii O, Kon Y. Vitamin A deprivation affects the progression of the spermatogenic wave and initial formation of the blood-testis barrier, resulting in irreversible testicular degeneration in mice. J Reprod Dev 2013; 59:525–535.
16. Huang HF, Marshall GR. Failure of spermatid release under various vitamin A states—an indication of delayed spermiation. Biol Reprod 1983; 28:1163–1172.
17. Bishop PD, Griswold MD. Uptake and metabolism of retinol in cultured Sertoli cells: evidence for a kinetic model. Biochemistry 1987; 26: 7511–7518.
18. Griswold MD, Bishop PD, Kim KH, Ping R, Siiteri JE, Morales C. Function of vitamin A in normal and synchronized seminiferous tubules. Ann N Y Acad Sci 1989; 564:154–172.
19. Morales C, Griswold MD. Retinol-induced stage synchronization in seminiferous tubules of the rat. Endocrinology 1987; 121:432–434.
20. Li H, Palczewski K, Baehr W, Clagett-Dame M. Vitamin A deficiency results in meiotic failure and accumulation of undifferentiated spermatogonia in prepubertal mouse testis. Biol Reprod 2011; 84:336–341.
21. Ghyselinck NB, Vernet N, Dennefeld C, Giese N, Nau H, Chambon P, Viville S, Retinoids Mark M. and spermatogenesis: lessons from mutant mice lacking the plasma retinol binding protein. Dev Dyn 2006; 235: 1608–1622.
22. Hogarth CA, Evanoff R, Mitchell D, Kent T, Small C, Amory JK, Griswold MD. Turning a spermatogenic wave into a tsunami: synchronizing murine spermatogenesis using WIN 18,446. Biol Reprod 2013; 88: 40.
23. Brooks NL, van der Horst G. Short-term effects of N′N-bis(dichloroacetyl)-1,8-octamethylenediamine (WIN 18446) on the testes, selected sperm parameters and fertility of male CBA mice. Lab Anim 2003; 37:363–373.
24. Raverdeau M, Gely-Pernot A, Feret B, Dennefeld C, Benoit G, Davidson I, Chambon P, Mark M, Ghyselinck NB. Retinoic acid induces Sertoli cell paracrine signals for spermatogonia differentiation but cell autonomously drives spermatocyte meiosis. Proc Natl Acad Sci U S A 2012; 109: 16582–16587.
25. Tong MH, Yang QE, Davis JC, Griswold MD. Retinol dehydrogenase 10 is indispensible for spermatogenesis in juvenile males. Proc Natl Acad Sci U S A 2013; 110:543–548.
26. Hogarth CA, Amory JK, Griswold MD. Inhibiting vitamin A metabolism as an approach to male contraception. Trends Endocrinol Metab 2011; 22: 136–144.
27. Hogarth CA, Griswold MD. Immunohistochemical approaches for the study of spermatogenesis. Methods Mol Biol 2013; 927:309–320.
28. Russell LD, Ettlin RA, Sinha Hikim AD. Histological EPC and histopathological evaluation of the testis. St. Louis, MO: Cache River Press; 1990.
29. van Beek ME, Meistrich ML. Stage-synchronized seminiferous epithelium in rats after manipulation of retinol levels. Biol Reprod 1991; 45:235–244.
30. Siiteri JE, Karl AF, Linder CC, Griswold MD. Testicular synchrony: evaluation and analysis of different protocols. Biol Reprod 1992; 46: 284–289.
31. Perez CV, Sobarzo CM, Jacobo PV, Pellizzari EH, Cigorraga SB, Denduchis B, Lustig L. Loss of occludin expression and impairment of blood-testis barrier permeability in rats with autoimmune orchitis: effect of interleukin 6 on Sertoli cell tight junctions. Biol Reprod 2012; 87:122.
32. Peters AH, Plug AW, van Vugt MJ, de Boer P. A drying-down technique for the spreading of mammalian meiocytes from the male and female germline. Chromosome Res 1997; 5:66–68.
33. Vrooman LA, Nagaoka SI, Hassold TJ, Hunt PA. Evidence for paternal age-related alterations in meiotic chromosome dynamics in the mouse. Genetics 2014; 196:385–396.
34. Amory JK, Muller CH, Shimshoni JA, Isoherranen N, Paik J, Moreb JS, Amory DW Sr, Evanoff R, Goldstein AS, Griswold MD. Suppression of spermatogenesis by bisdichloroacetyldiamines is mediated by inhibition of testicular retinoic acid biosynthesis. J Androl 2011; 32:111–119.
35. Hogarth CA, Griswold MD. Retinoic acid regulation of male meiosis. Curr Opin Endocrinol Diabetes Obes 2013; 20:217–223.
36. Hogarth CA, Evanoff R, Snyder E, Kent T, Mitchell D, Small C, Amory JK, Griswold MD. Suppression of Stra8 expression in the mouse gonad by WIN 18,446. Biol Reprod 2011; 84:957–965.
37. Topping D, Brown P, Judis L, Schwartz S, Seftel A, Thomas A, Hassold T. Synaptic defects at meiosis I and non-obstructive azoospermia. Hum Reprod 2006; 21:3171–3177.
38. de Vries FA, de Boer E, van den Bosch M, Baarends WM, Ooms M, Yuan L, Liu JG, van Zeeland AA, Heyting C, Pastink A. Mouse Sycp1 functions in synaptonemal complex assembly, meiotic recombination, and XY body formation. Genes Dev 2005; 19:1376–1389.
39. Heller CG, Moore DJ, Paulsen CA. Suppression of spermatogenesis and chronic toxicity in men by a new series of bis(dichloroacetyl) diamines. Toxicol Appl Pharmacol 1961; 3:1–11.
40. Heller CG, Flageolle BY, Matson LJ. Histopathology of the human testes as affected by bis(dichloroacetyl)diamines. Exp Mol Pathol Suppl 1963; 2: 107–114.
41. Coulston F, Beyler AL, Drobeck HP. The biologic actions of a new series of bis(dichloroacetyl) diamines. Toxicol Appl Pharmacol 1960; 2: 715–731.
42. Beyler AL, Potts GO, Coulston F, Surrey AR. The selective testicular effects of certain bis-(dichloroacetyl) diamines. Endocrinology 1961; 69: 819–833.
43. Asa C, Zaneveld LJD, Munson L, Callahan M, Byers AP. Efficacy, safety and reversibility of a bisdiamine male-directed oral contraceptive in grey wolves (*Canis lupus*). J Zoo Wildl Med 1996; 27:501–506.
44. Munson L, Chassy LM, Asa C. Efficacy, safety and reversibility of bisdiamine as a male contraceptive in cats. Theriogenology 2004; 62: 81–92.
45. Singh SK, Dominic CJ. Effect of N,N′-bis(dichloroacetyl)-i,8-octamethylenediamine (WIN 18446) on the testis + epididymis of the musk shrew *Suncus murinus* L. Indian J Exp Biol 1980; 18:1217–1220.
46. Gely-Pernot A, Raverdeau M, Celebi C, Dennefeld C, Feret B, Klopfenstein M, Yoshida S, Ghyselinck NB, Mark M. Spermatogonia differentiation requires retinoic acid receptor gamma. Endocrinology 2012; 153:438–449.
47. Snyder EM, Davis JC, Zhou Q, Evanoff R, Griswold MD. Exposure to retinoic acid in the neonatal but not adult mouse results in synchronous spermatogenesis. Biol Reprod 2011; 84:886–893.
48. Davis JC, Snyder EM, Hogarth CA, Small C, Griswold MD. Induction of spermatogenic synchrony by retinoic acid in neonatal mice. Spermatogenesis 2013; 3:e23180.
49. Saitou M, Furuse M, Sasaki H, Schulzke JD, Fromm M, Takano H, Noda T, Tsukita S. Complex phenotype of mice lacking occludin, a component of tight junction strands. Mol Biol Cell 2000; 11:4131–4142.
50. Kubota H, Chiba H, Takakuwa Y, Osanai M, Tobioka H, Kohama G, Mori M, Sawada N. Retinoid X receptor alpha and retinoic acid receptor gamma mediate expression of genes encoding tight-junction proteins and barrier function in F9 cells during visceral endodermal differentiation. Exp Cell Res 2001; 263:163–172.
51. Nicholls PK, Harrison CA, Rainczuk KE, Wayne Vogl A, Stanton PG. Retinoic acid promotes Sertoli cell differentiation and antagonises activin-induced proliferation. Mol Cell Endocrinol 2013; 377:33–43.
52. Chung SS, Choi C, Wang X, Hallock L, Wolgemuth DJ. Aberrant distribution of junctional complex components in retinoic acid receptor alpha-deficient mice. Microsc Res Tech 2010; 73:583–596.
53. Endo T, Romer KA, Anderson EL, Baltus AE, De Rooij DG, Page DC. Periodic retinoic acid-STRA8 signaling intersects with periodic germ-cell competencies regulate spermatogenesis. Proc Natl Acad Sci U S A 2015; 112:E2347–E2356.
54. Lin M, Napoli JL. cDNA cloning and expression of a human aldehyde dehydrogenase (ALDH) active with 9-*cis*-retinal and identification of a rat ortholog, ALDH12. J Biol Chem 2000; 275:40106–40112.
55. Wu JW, Wang RY, Guo QS, Xu C. Expression of the retinoic acid-metabolizing enzymes RALDH2 and CYP26b1 during mouse postnatal testis development. Asian J Androl 2008; 10:569–576.
56. Fan X, Molotkov A, Manabe S, Donmoyer CM, Deltour L, Foglio MH,

Cuenca AE, Blaner WS, Lipton SA, Duester G. Targeted disruption of Aldh1a1 (Raldh1) provides evidence for a complex mechanism of retinoic acid synthesis in the developing retina. Mol Cell Biol 2003; 23: 4637–4648.
57. Evans E, Hogarth C, Mitchell D, Griswold M. Riding the spermatogenic wave: profiling gene expression within neonatal germ and Sertoli cells during a synchronized initial wave of spermatogenesis in mice. Biol Reprod 2014; 90:108.
58. Napoli JL. Retinol metabolism in LLC-PK1 cells: characterization of retinoic acid synthesis by an established mammalian cell line. J Biol Chem 1986; 261:13592–13597.
59. Adams MK, Belyaeva OV, Wu L, Kedishvili NY. The retinaldehyde reductase activity of DHRS3 is reciprocally activated by retinol dehydrogenase 10 to control retinoid homeostasis. J Biol Chem 2014; 289:14868–14880.
60. Billings SE, Pierzchalski K, Butler Tjaden NE, Pang XY, Trainor PA, Kane MA, Moise AR. The retinaldehyde reductase DHRS3 is essential for preventing the formation of excess retinoic acid during embryonic development. FASEB J 2013; 27:4877–4889.
61. Kam RK, Shi W, Chan SO, Chen Y, Xu G, Lau CB, Fung KP, Chan WY, Zhao H. Dhrs3 protein attenuates retinoic acid signaling and is required for early embryonic patterning. J Biol Chem 2013; 288:31477–31487.
62. Sandell LL, Lynn ML, Inman KE, McDowell W, Trainor PA. RDH10 oxidation of vitamin A is a critical control step in synthesis of retinoic acid during mouse embryogenesis. PLoS One 2012; 7:e30698.
63. Ruiz A, Winston A, Lim YH, Gilbert BA, Rando RR, Bok D. Molecular and biochemical characterization of lecithin retinol acyltransferase. J Biol Chem 1999; 274:3834–3841.
64. Hogarth CA, Griswold MD. The key role of vitamin A in spermatogenesis. J Clin Invest 2010; 120:956–962.